Two-Component Non-Collinear Time-Dependent Spin Density Functional Theory for the Excited States Calculations

Franco Egidi,[†] Shichao Sun,[†] Joshua J. Goings,[†] Giovanni Scalmani,[‡] Michael J. Frisch,[‡] and Xiaosong Li[*,†]

†*Department of Chemistry, University of Washington, Seattle, WA, 98195*

‡*Gaussian Inc., 340 Quinnipiac St, Bldg 40, Wallingford, CT, USA 06492*

E-mail: xsli@uw.edu

Abstract

We present a linear response formalism for the description of the electronic excitations of a non-collinear reference defined via Kohn-Sham spin density functional methods. A set of auxiliary variables, defined using the density and non-collinear magnetization density vector, allows the generalization of spin density functional kernels commonly used in collinear DFT to non-collinear cases, including local density, GGA, meta-GGA and hybrid functionals. Working equations and derivations of functional second derivatives with respect to the non-collinear density, required in the linear response non-collinear TDDFT formalism, are presented in this work. This formalism takes all components of the spin magnetization into account independent of the type of reference state (open or closed shell). As a result, the method introduced here is able to afford a non-zero local *xc* torque on the spin magnetization, while still satisfying the zero-torque theorem globally. The formalism is applied to a few test cases using the

variational exact-two-component reference including spin-orbit coupling to illustrate the capabilities of the method.

1 Introduction

In recent years we have witnessed an ever expanding research effort in the modeling of spin-related phenomena, which are at the basis of magnetic materials and spintronic devices.[1–4] An accurate theoretical description of the variety of spin phenomena involved in these fields requires enough flexibility to allow the spin magnetization vector to move about and re-orient itself along any axis. In some cases, the direction of the spin magnetization may not be the same at every point in space, a situation often referred to as non-collinear spin. This flexibility in the spin orientation is unfortunately not found in most common quantum chemical methods, which implicitly assume that the spin magnetization is uniformly oriented along an axis, conventionally taken to be the z axis. Therefore, generalizations of widely available theoretical and computational methods specifically designed to describe these spin arrangements are greatly appreciated.

Non-collinear spins also have a prominent role in relativistic quantum chemical theory based on the Dirac equation.[5,6] Relativistic effects are known to be of importance for the description of heavy elements, in which *scalar* relativistic effects cause significant contractions of the core electron shells,[7] but they also introduce spin-spin and spin-orbit couplings in the Hamiltonian, whose effects can be observed directly even in light atoms in the fine structure splittings that occur in their ground and excited electronic states. While scalar relativistic effects can be modeled using a collinear method, the introduction of spin-orbit couplings often requires this constraint to be relaxed so that a more consistent description of the system can be achieved. This is not merely academic: a growing class of multiferroics are functional strictly due to the noncollinear arrangement of their lattice spins.[8] The relativistic corrections to the Heisenberg exchange interaction due to spin orbit coupling, known as

the Dzyaloshinskii-Moriya interaction,[9,10] favor perpendicular orientations of adjacent spins leading to an overall noncollinear spin orientation (often called a spiral magnetic order). This leads to magnetic ferroelectric materials with an extreme sensitivity to external magnetic fields.

Among the quantum chemical methods that are available today, density functional theory (DFT) has become the method of choice for a wide array of applications thanks to its ability to offer a good compromise between accuracy and computational cost. It is therefore highly desirable to extend the method based on DFT to the non-collinear framework. Unfortunately, density functionals commonly employed in quantum chemistry have been developed for collinear densities, and therefore there is no straightforward way to employ them in non-collinear systems. Ideally, new density functionals specifically designed to take non-collinearity into account should be used, and some work has be done in this direction.[11] However, for the time being it would be highly desirable to use standard functionals in non-collinear DFT. The results of many benchmarking studies have shown that these functionals yield accurate results in a wide variety of contexts and for the calculation of a multitude of molecular properties.

Several different approaches have been proposed to address this problem,[12–29] and in this work we extend a non-collinear DFT formalism previously applied for ground-state calculations[19–21] to the description of excited states, and built upon previous work by some of us on excited-state two-component methods such as the time-dependent Hartree-Fock (2c-TDHF) method[30,31] and the particle-particle Tamm-Dancoff approximation.[32] The approach presented here is compatible with the inclusion of relativistic effects such as spin-orbit coupling *via* one of the many available methods such as the Douglas-Kroll-Hess expansion to 4th order,[33–35] the normalized elimination of the small components,[36,37] or the exact two-component method (X2C).[24,25,31,38–48]

2 Theory

2.1 Two-component Relativistic Hamiltonian

The Dirac Hamiltonian in relativistic quantum mechanics has the following expression:[5,6]

$$\hat{\mathcal{H}} = \begin{pmatrix} V\sigma_0 & c\boldsymbol{\sigma}\cdot\mathbf{p} \\ c\boldsymbol{\sigma}\cdot\mathbf{p} & (V-2mc^2)\sigma_0 \end{pmatrix} \tag{1}$$

where V is the scalar potential, $\boldsymbol{\sigma}$ is a vector whose components are the Pauli matrices, and σ_0 is the rank-two identity matrix. The relativistic wave function is a four-component (4c) object, and is usually separated into the large and small components which each consists of spin-up and spin-down parts:

$$\psi^{4c} = \begin{pmatrix} \psi_{\mathrm{L}} \\ \psi_{\mathrm{S}} \end{pmatrix} \tag{2}$$

$$\psi_{\mathrm{L}} = \begin{pmatrix} \psi_{\mathrm{L}}^{\alpha} \\ \psi_{\mathrm{L}}^{\beta} \end{pmatrix} \quad ; \quad \psi_{\mathrm{S}} = \begin{pmatrix} \psi_{\mathrm{S}}^{\alpha} \\ \psi_{\mathrm{S}}^{\beta} \end{pmatrix} \tag{3}$$

In the non-relativistic limit, for positive-energy solutions, the large component approaches the non-relativistic wave function while the small component vanishes. From the four-component wave function, the spin density can be obtained through the Gordon decomposition of the three-current:[26,49]

$$\mathbf{s} = \frac{1}{2}\psi^{\dagger}\beta\boldsymbol{\Sigma}\psi \quad ; \quad \beta\boldsymbol{\Sigma} = \begin{pmatrix} \boldsymbol{\sigma} & 0_2 \\ 0_2 & -\boldsymbol{\sigma} \end{pmatrix} \tag{4}$$

While the Dirac equation can be solved in its full form, it is often convenient to simplify it by transforming it into a form that is closer to its non-relativistic counterpart. This is

achieved by means of a unitary transformation $\mathcal{U}$ such that:

$$\mathcal{U}\hat{\mathcal{H}}\mathcal{U}^\dagger = \begin{pmatrix} \hat{H}_+ & \mathbf{0}_2 \\ \mathbf{0}_2 & \hat{H}_- \end{pmatrix} \quad ; \quad \mathcal{U}\begin{pmatrix} \psi_\mathrm{L} \\ \psi_\mathrm{S} \end{pmatrix} = \begin{pmatrix} \psi^\mathrm{2c} \\ 0 \end{pmatrix} \tag{5}$$

The two-component transformed wave function is an eigenstate of the transformed Hamiltonian operator $\hat{H}_+$. Given its two-component form, the transformed Dirac equation can be solved using techniques that are also employed in the case of non-collinear non-relativistic quantum chemistry.[23,25–27,48] The exact transformation $\mathcal{U}$ for the full equation including the two-electron terms cannot, however, be found in most practical cases. Therefore, one must introduce approximations for the decoupling of the large and small components. In this contribution we will employ the the exact two-component method (X2C), where the appellative "exact" refers to the fact that X2C is based on the exact diagonalization of the one-electron four-component Hamiltonian,[24,25,29,31,32,38,40–45] though the term X2C can also be used more in general to describe methods in which an effective Hamiltonian, such as a mean-field Dirac-Fock operator, is diagonalized to obtain a suitable two-component one-electron operator.[39,40,46,47] A very common approximation is to neglect the transformation of the two-electron terms of the Dirac Hamiltonian. This approach greatly reduces the computational cost associated with the transformation, but it neglects two-electron spin-orbit terms, some of which are of the same order as their one-electron counterparts. Several methods have been proposed to recover *a posteriori* the effect of the two-electron spin-orbit contributions.[24,37,42,50] Here we adopt a simple method that uses a fudging of the one-electron spin-orbit terms according to a scheme that takes the angular momentum of the functions into account.[51,52]

2.2 Two-component Density Functional Theory

Non-relativistic density functional theory is based on the Hohenberg-Kohn theorem and it is realized in quantum chemistry through the Kohn-Sham method. The same approach

can be carried over to the relativistic framework provided that the density is replaced with the ground-state four-current.[53–55] While the exact relativistic functional may depend on the current, in most practical applications this dependence is dropped in favor of a simpler dependence on the electron density only. Even with this simpler density dependence, density functionals commonly used in quantum chemistry implicitly assume that density to be collinear, i.e. that the spin magnetization is oriented along the same axis (conventionally chosen to be the z axis) at all points in space. This situation is usually acceptable in the non-relativistic regime, with an exception given by spin-frustrated systems. However, fundamental relativistic effects such as the presence of spin-orbit coupling in the Dirac equation can cause the magnetization to assume a non-collinear configuration. The development of true non-collinear density functionals that depend on both the total density and the magnetization vector density is an ongoing effort.[11] However, a common approach is to reformulate the density-dependence of collinear functionals in order to use them in a non-collinear two-component Kohn-Sham method. This extension allows one to benefit from the rich development in the field of collinear non-relativistic DFT made in the last few decades.[12–28,56]

In the two-component formalism the generalized density can be expressed in a spin-blocked form or as a sum of the total density n and the vector magnetization density $\mathbf{m}$:

$$\rho(\mathbf{r}) = \begin{pmatrix} \rho^{\alpha\alpha}(\mathbf{r}) & \rho^{\alpha\beta}(\mathbf{r}) \\ \rho^{\beta\alpha}(\mathbf{r}) & \rho^{\beta\beta}(\mathbf{r}) \end{pmatrix} = \frac{1}{2} n(\mathbf{r}) \sigma_0 + \frac{1}{2} \mathbf{m}(\mathbf{r}) \circ \boldsymbol{\sigma} \tag{6}$$

where the circle '$\circ$' is used to denote a scalar product over the magnetization spin labels of any two quantities ($\mathbf{a} \circ \mathbf{b} = \sum_{k=x,y,z} a_k b_k$). The expressions of the density elements can be found in the Appendix.

A strictly local exchange-correlation functional would require only these density variables to be considered. However, more advanced density functionals capable of achieving more accurate results, also depend on the density gradients, the Laplacian of the densities or the

kinetic energy densities. In order to make use of such functional forms in the relativistic two-component Kohn-Sham method, the functionals are redefined (in the similar spirit of spin-polarized DFT) to depend on a set of auxiliary generalized variables which take the full magnetization vector density into account,[19–21]

$$E_{\mathrm{xc}} = \int f(n_+, n_-, \gamma_{++}, \gamma_{--}, \gamma_{+-}, \tau_+, \tau_-)\, \mathrm{d}\,\mathbf{r} \tag{7}$$

where the generalized variables are defined as follows

$$\begin{aligned}
n^{\pm} &= \frac{1}{2} n \pm \frac{1}{2}\sqrt{\mathbf{m} \circ \mathbf{m}} \\
\gamma^{\pm\pm} &= \frac{1}{4}\boldsymbol{\nabla} n \cdot \boldsymbol{\nabla} n + \frac{1}{4}\boldsymbol{\nabla}\mathbf{m} \cdot \circ \boldsymbol{\nabla}\mathbf{m} \pm \frac{f_\nabla}{2}\sqrt{\boldsymbol{\nabla} n \cdot \boldsymbol{\nabla}\mathbf{m} \circ \boldsymbol{\nabla}\mathbf{m} \cdot \boldsymbol{\nabla} n} \\
\gamma^{+-} &= \frac{1}{4}\boldsymbol{\nabla} n \cdot \boldsymbol{\nabla} n - \frac{1}{4}\boldsymbol{\nabla}\mathbf{m} \cdot \circ \boldsymbol{\nabla}\mathbf{m} \\
\tau^{\pm} &= \frac{1}{2}\tau \pm \frac{f_{\mathbf{u}}}{2}\sqrt{\mathbf{u} \circ \mathbf{u}} \\
f_\nabla &= \mathrm{sgn}(\boldsymbol{\nabla} n \cdot \boldsymbol{\nabla}\mathbf{m} \circ \mathbf{m}) \\
f_{\mathbf{u}} &= \mathrm{sgn}(\mathbf{u} \circ \mathbf{m})
\end{aligned} \tag{8}$$

In the expression above τ and $\mathbf{u}$ are the total and magnetization vector kinetic energy densities, while 'sgn' indicates the sign function. For meta-GGA, additional Laplacians of the densities are needed (see the Appendix).[20]

These definitions have the advantage of yielding an energy that is independent of the choice of the global orientation of the magnetization. Compared to other definitions of the generalized density variables,[13–17,22,23,25–27] the method proposed herein, when applied to non-local functionals, can yield a non-zero local torque acting on the magnetization while still giving rise to a zero global torque. This property satisfies the zero-torque theorem, which is a known property of the exact functional.[57] It should be pointed out that the exact functional in Eq. (7) is not formally the same as the exact density functional that should be used in the time-dependent theory. In this work, we choose to generalize the common practice of

employing the same functional for both ground state and response calculations to the regime of non-collinear spins. In addition, we cast our formalism within the generalized Kohn-Sham (GKS) formalism, in which no restrictions are imposed on the the density in terms of spin, and allows to model bond-breaking without resorting to multi-reference methods. This is in contrast with recent developments in spin-adapted TDDFT,[28,58] which have the advantage of avoiding spin-contamination problems in open-shell system.

2.3 Functional Derivatives of Non-Collinear DFT

In deriving the linear response equation for non-collinear DFT, derivatives of the functional up to second order with respect to the density variables must be evaluated. Mathematical derivations of functional derivatives with respect to fundamental density variables and their working equations in atomic orbital basis are presented in the Appendix. These equations have been implemented in this work for a large class of functionals, including GGAs and functionals that depend on the kinetic energy density and the Laplacian of the density. In this section, we only highlight technical details that addresses some challenges in developing functional second derivatives for non-collinear DFT.

Derivatives of a functional, which is defined in terms of auxiliary variables, with respect to fundamental density matrix elements can be obtained by the application of chain rules. While expressions for the functional derivatives with respect to the auxiliary variables have the same forms as for the collinear case, the derivatives of auxiliary variables with respect to density variables, e.g. $\frac{\partial n^+}{\partial \mathbf{m}}$ and $\frac{\partial^2 n^+}{\partial \mathbf{m} \partial \mathbf{m}}$, are very different (see the Appendix). Complications may however arise in regions where the magnetization is zero or close to zero, especially in the case of second derivatives. This is apparent in the expression for some of the chain rule coefficients. For instance,

$$\frac{\partial^2 n^+}{\partial \mathbf{m} \partial \mathbf{m}} = \frac{1}{m} \left(1 - \frac{\mathbf{m} \otimes \mathbf{m}}{m^2} \right) \tag{9}$$

when m is close to zero, such as in regions where magnetization is very small, however, this quantity can be ill-conditioned within a given machine precision, and the magnetization vector becomes directionless. Although such situation can be easily avoided for a perfectly closed shell system,[14–16] it imposes a challenge to the development of numerically stable non-collinear DFT methods for open-shell systems.

In this work, we wish to develop a general and numerically stable method that is applicable for any reference state (open or closed shell) and in which the magnetization may possibly be zero (or very small) in some regions of space, and non-zero in others. A crucial aspect of the development is ensuring that the first and second functional derivatives are numerically stable, even when the direction of the magnetization may be effectively discontinuous in regions where its magnitude is very small.

Numerical instabilities arise from the functional differentiation with respect to magnetization vector and magnetization vector kinetic energy densities in the square-root form (see Eq. (8)). To avoid having the magnetization length m in the denominator of functional derivatives, we choose to use scalar forms of magnetization vector and magnetization vector kinetic energy densities in the square-root terms only in regions where the magnetization length is below a threshold ($m < 10^{-12}$ used in this work). This leads to slightly different auxiliary variables,

$$\begin{aligned}
n^{\pm} &= \frac{1}{2}n \pm \frac{1}{2}m_s \\
\gamma^{\pm\pm} &= \frac{1}{4}\boldsymbol{\nabla} n \cdot \boldsymbol{\nabla} n + \frac{1}{4}\boldsymbol{\nabla}\mathbf{m} \cdot \circ \boldsymbol{\nabla}\mathbf{m} \pm \frac{f_{\nabla}}{2}\boldsymbol{\nabla} n \cdot \boldsymbol{\nabla} m_s \\
\gamma^{+-} &= \frac{1}{4}\boldsymbol{\nabla} n \cdot \boldsymbol{\nabla} n - \frac{1}{4}\boldsymbol{\nabla}\mathbf{m} \cdot \circ \boldsymbol{\nabla}\mathbf{m} \\
\tau^{\pm} &= \frac{1}{2}\tau \pm \frac{f_{\mathbf{u}}}{2}u_s \\
m_s &= \frac{1}{3}(m_x + m_y + m_z) \\
u_s &= \frac{1}{3}(u_x + u_y + u_z)
\end{aligned} \tag{10}$$

The advantage of this formulation is that square-root terms that lead to the near-zero de-

nominators in the chain rule coefficients disappear, while the equations still approach the correct limit for zero magnetization. It seems that this alternate definition of auxiliary variables breaks the invariance with respect to rotations of the spin reference frame. However, as long as it is used only in regions where the magnetization is small enough, such properties are still satisfied numerically to an acceptable accuracy. The validity of the present approximation has been tested on several systems, and results are outlined in the following sections.

2.4 AO Direct Linear Response Formalism of Non-collinear TDDFT

The linear response formalism of the time-dependent two-component Hartree-Fock method has been derived and discussed in the previous work.[31,59] Although they are fundamentally different, the working equations of two-component TDDFT and TDHF in the molecular orbital (MO) basis share a similar matrix representation,

$$\begin{pmatrix} \mathbf{A} & \mathbf{B} \\ \mathbf{B}^* & \mathbf{A}^* \end{pmatrix} \begin{pmatrix} X \\ Y \end{pmatrix} = \omega \begin{pmatrix} 1 & 0 \\ 0 & -1 \end{pmatrix} \begin{pmatrix} X \\ Y \end{pmatrix} \tag{11}$$

where X and Y represent the excitation and de-excitation amplitudes. The matrices $\mathbf{A}$ and $\mathbf{B}$ are defined as:

$$A_{ai,bj} = \delta_{ab}\delta_{ij}(\varepsilon_a - \varepsilon_i) + K_{ai,bj} \tag{12}$$

$$B_{ai,bj} = K_{ai,jb} \tag{13}$$

For non-collinear TDDFT, the coupling matrix $\mathbf{K}$ depends on the form of exchange and correlation functionals and functional derivatives. Note that Eq. (11) is cast in the X2C transformed picture frame.[31] For discussions on the effect of two-component picture frame change on excitation energies, we refer readers to Ref. 31. Also note that Eq. (11) is closely related to the stability test of two-component ground state wave function.[59–61]

Equation (11) is a complex non-Hermitian eigenvalue equation of dimension $2\mathcal{OV}$, which is usually solved numerically using the Davidson algorithm,[62] since only the lowest few excited states are typically needed. Higher energy states can be obtained in a similar way using energy-windowed algorithms.[63,64] Given the high dimensionality that both the linear response and stability problems can reach, the matrix vector products in Eq. (11) are performed in a direct fashion in the AO basis. The details of the efficient direct contraction algorithm of the Coulomb and HF exchange terms have been discussed in an earlier contribution.[31] In this paper, we focus on direct contraction algorithm with the non-collinear transition density related to functional derivatives that occur in the coupling matrix.

The coupling matrix in the AO basis has the following general expression,

$$K_{\mu\nu,\kappa\lambda} = (\mu\nu|\kappa\lambda) + \frac{\partial^2 E_{\mathrm{xc}}}{\partial P_{\mu\nu}\partial P_{\kappa\lambda}} \tag{14}$$

The working equations for the functional second derivatives in non-collinear density matrix basis are derived and presented in the Appendix. The direct algorithm using Davidson type of solvers to solve Eq. (11) requires the on-the-fly contraction of four-index coupling matrix elements (Eq. (14)) with the two-component non-Hermitian transition density, $\mathbf{T}$ obtained by transforming the guess vector $|X\,Y\rangle$ into the AO basis, to form the matrix-vector product on the left hand side of Eq. (11). Detailed technical aspects regarding this direct contraction step and procedure to reduce the computational costs are discussed in the Appendix.

3 Applications

All calculations were performed with a locally modified version of the Gaussian quantum chemistry program package.[65] Relativistic effects were accounted for by means of the X2C method.[24,25,38,40–42] In order to partially account for two-electron spin-orbit interactions in the Hamiltonian, we employed a scheme based on the scaling of the one-electron interactions depending on the nuclear charges and the angular momenta of the basis functions involved.[51]

The atomic nuclei, rather than being treated as point charges, were described using s-type functions.[66,67] The stability of the ground state wave function was also tested before linear response calculations were performed. For the various examples in the following subsections, we used the LSDA,[68,69] BLYP,[70–72] B3LYP,[71,73] PBE,[74] PBE0,[75] TPSS,[76] M06-2X,[77] and M06-HF[78,79] functionals.

3.1 Dilithium

To illustrate the features of the method we present in this subsection results on the dilithium molecule. This system has been extensively studied using a variety of theoretical methods in the past,[80–94] and its small size allows for extensive testing. It is well known that methods restricting the spin pairing of the electrons, such as restricted Hartree-Fock (RHF) and its Kohn-Sham equivalents, cannot be used to produce potential energy surfaces of dissociating systems correctly. This is because, for instance, while the system is in a singlet state at the equilibrium geometry, as bonds are broken the triplet reference state may become more stable. Being able to employ an unrestricted reference is helpful in these cases. Just like in the unrestricted Hartree-Fock (UHF) method, however, a non-zero spin multiplicity in the single-determinant ground state causes the excited states to be spin-contaminated.[95]

As a simple model system to study the effect of bond-breaking on the excited states, we calculated the potential energy surfaces of the lowest excited states of dilithium using the linear response two-component non-collinear TDDFT method developed in this work at the 2c-B3LYP/Sapporo-DZP-2012[96] level of theory with relativistic effects in the description (shown in Fig. 1). Since lithium is a very light atom, spin-orbit couplings are too small to cause a significant degree of non-collinearity and spin is still a good quantum number. Nevertheless, it is still an interesting system to study because the ground state reference within a single determinant description undergoes a continuous transition from a closed shell to an open shell configuration as the bond breaks. This correlates to the change of definition of the auxiliary variables from Eq. (10) to Eq. (8) as the magnetization increases

from zero (closed shell) to 2 (open shell).

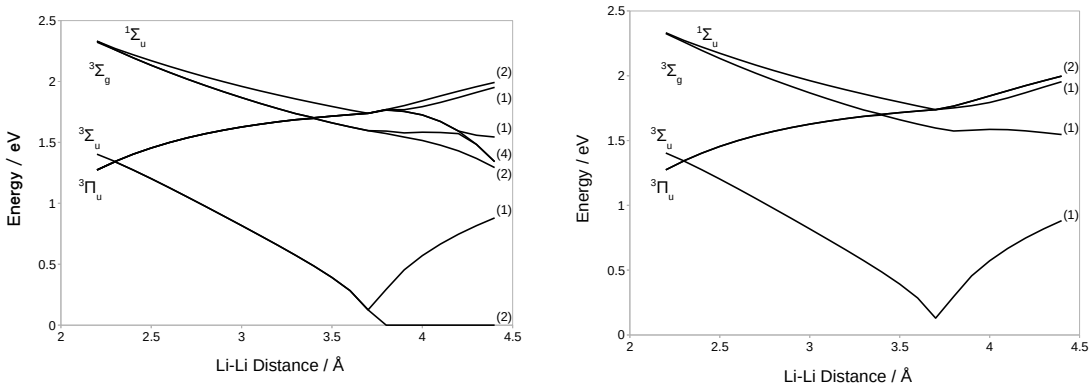

Figure 1. Left: 2c-B3LYP excitation energies as a function of Li-Li bond length. **Right:** UB3LYP excitation energies as a function of Li-Li bond length. Numbers in parenthesis indicate degeneracy.

At small interatomic distances the ground state of the system has a closed shell configuration $^1\Sigma_g$ with no significant degree of non-collinearity, and the excited states also have well-defined symmetries and spin multiplicities. The energy levels computed at 2c-B3LYP in this region are the same as those computed at UB3LYP. However, UB3LYP results miss a number of degenerate states within a same spin manifold due to the restricted spin alignment.[59] This is due to the fact that in the one-component calculations we are not converging any of the spin-flip states, and for each triplet manifold only the state with $m_s = 1$ is converged. At the bond length of $\sim$3.8 Å, the ground state undergoes a reference change from closed-shell to open-shell. As a result, excited state potential energy surfaces intersect in that region. The triple degenerate ground state is correctly captured in the 2c-B3LYP calculations. For detailed discussions regarding spin-symmetry characteristics of two-component methods for excited state calculations, please see Ref. 59.

This simple test suggests that the change of definition of auxiliary variables in the situation of small magnetization does not introduce a discontinuity in the excited state potential energy surfaces within the numerical accuracy.

3.2 Trilithium

In this section we analyze the excited states of a lithium trimer model system, which has been extensively studied in the literature[97–103] and was shown to have non-collinear states even in the absence of relativistic effects.[30] The non-collinearity of each electronic state can be visualized as local magnetization vector on each atom using the Hirshfeld partitioning scheme.[104] In a collinear solution all vectors would be oriented along the same (arbitrary) direction. For the excited state, the Hirshfeld partitioning scheme is applied to analyze the unrelaxed excited state density matrix defined as[95,105,106]

$$P^{\mathrm{exc}}_{pq} = P^{0}_{pq} + \sum_{i}^{\mathrm{occ}} (X^{*}_{pi} X_{qi} + Y^{*}_{pi} Y_{qi}) - \sum_{a}^{\mathrm{vir}} (X^{*}_{ap} X_{aq} + Y^{*}_{ap} Y_{aq}) \tag{15}$$

where $\mathbf{P}^0$ is the ground-state density, and X and Y are the excitation and de-excitation amplitudes. The calculated local magnetization vectors of excited states and their energies using 2c-PBE are shown in Fig. 2.

We consider this molecule in an equilateral triangular geometry (D_{3h} symmetry), with a bond distance of 4.0 Å. The ground state has a four-fold degeneracy with different alignments of local magnetization vectors shown as the red-arrows and States 1–3 in Fig. 2). This is expected from (Hartree-Fock) studies on similar noncollinear systems.[59,61,107] These ground state wave functions have been confirmed to be stable.[61] In the presented calculations, the reference for linear response calculations corresponds to a non-collinear arrangement of magnetization vectors when three local vectors are pointing outwards with 120° angle with respect to each other (see red-arrows in Fig. 2). Note that approximate treatment of 2c-TDDFT, such as the Tamm-Dancoff approximation, can not reproduce degenerate non-collinearity due to the lack of de-excitation amplitudes. All non-collinear DFT functionals (2c-LSDA, 2c-PBE and 2c-PBE0) tested herein produce similar state orderings. For detailed analysis of energetic and symmetry characteristics of molecules with D_{3h} symmetry in a non-collinear formalism, we refer readers to Ref. 59.

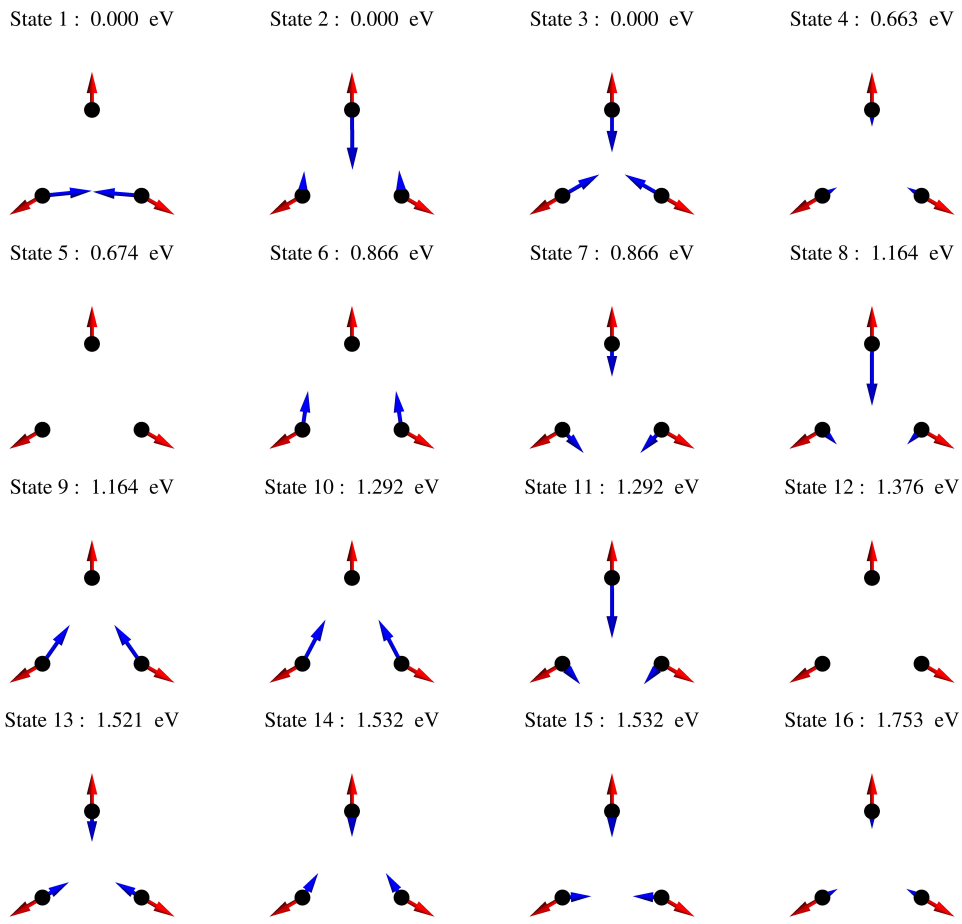

Figure 2. Hirshfeld magnetization vectors of the reference state (red arrows) and the 2c-PBE calculated states (blue arrows) of Li_3.

Figure 2 suggests that the auxiliary variables defined in this work give rise to the correct physics — non-zero local magnetizations while still being a non-collinear system and having a zero global magnetization (e.g. States 1-5 in Fig. 2). It is also worth mentioning that the linear response two-component non-collinear DFT methods allow change of global magnetization upon excitation as exemplified by the non-zero global spin-projection for states 6 to 11.

The strongly non-collinear solution of the lithium trimer allows for a good test of the correctness of our implementation of the functional second derivatives, by comparing the absorption spectra obtained by LR-2c-TDDFT with the same spectra obtained with real-time two-component time-dependent density functional theory (RT-2c-TDDFT).[29,30] The two methods are equivalent when used to obtain electronic absorption spectra. However, RT-2c-TDDFT does not require the explicit evaluation of functional second derivatives, and therefore if our derivation and implementation of the functional second derivatives is correct, the two methods should agree. We show a comparision of the absorption spectrum of the lithium trimer for the two methods using the PBEPBE exchange-correlation functional in Fig. 3. The stick spectra from LR-2c-TDDFT is overlaid on the absorption lineshape is from the RT calculations. The RT solution was perturbed with a delta electric field pulse of 0.005 $\mathrm{V{\cdot}\AA^{-1}}$ and propagated for 40 fs with time step of 0.000242 fs (0.01 au) using the second-order modified midpoint unitary method (MMUT).[108–110] To accelerate the convergence of the Fourier transform, we used the Padé transformation scheme,[111] and the electric dipole response was damped exponentially to give each peak a Lorentzian line shape with full-width half-max of 0.03 eV. Though the real time methods can only resolve optically bright modes, we see excellent agreement between the two methods. For the lowest six peaks considered, the maximum deviation between the two methods is 0.01 eV, with a mean absolute error of 0.002 eV. The discrepancies are due to the numerical integration error from the finite time step used in the RT calculations. Though the peak heights are arbitrarily scaled for comparison between the methods, we find it encouraging that relative peak height is consistent among

the LR and RT methods.

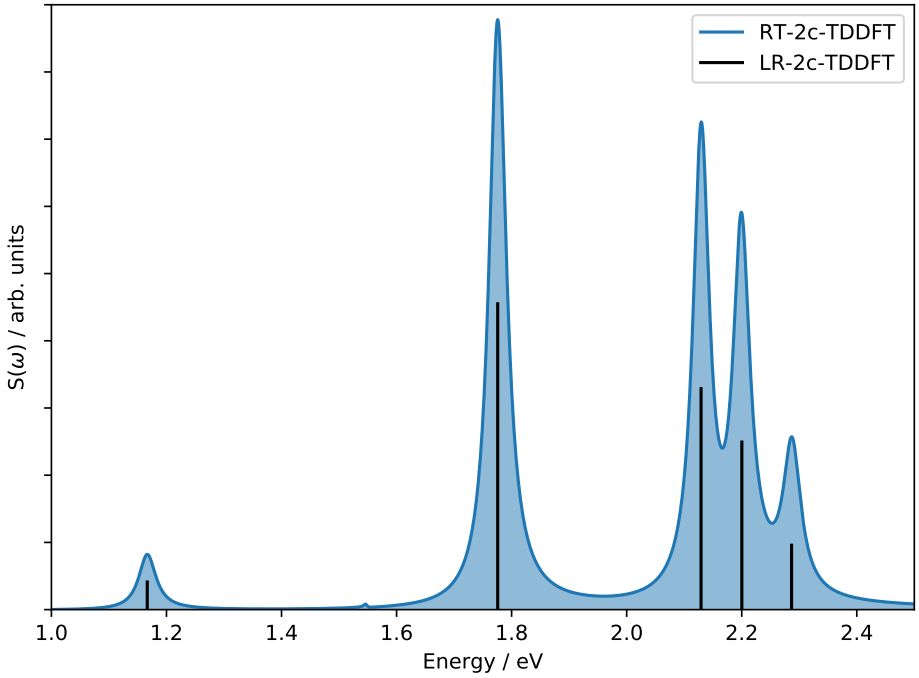

Figure 3. Comparison of the computed optical absorption spectra of noncollinear Li_3 between the linear response (stick plot) and real time TDDFT (line shape) formalisms with the PBEPBE exchange-correlation functional. The excellent agreement of the two methods indicate the correctness of the LR functional second derivatives, as RT methods do not require the explicit calculation of functional second derivatives, and the RT and LR methods access the same fundamental observables. For the peaks considered, the mean absolute deviation is 0.002 eV, which is within numerical error for the finite timestep used in RT-2c-TDDFT. Details of the RT calculation can be found in the text.

3.3 Uranyl Ion

In this section we turn our attention to a more realistic and chemically interesting system, the linear uranyl(VI) ion UO_2^{2+}. This is molecule has been studied in earlier work using different electronic structure methods, including methods employing perturbative treatment of spin-orbit couplings.[22,31,112–116] This system has an even number of electrons, and would give a singlet ground state in a non-relativistic framework. For our tests we selected a U-O bond distance of 1.708 Å. When spin-orbit couplings are introduced in the two-component non-collinear formalism, the variational optimization of the ground state Kohn-Sham determinant

yields a state with a non-zero total spin expectation value. In addition, spin-orbit couplings also cause splittings in the excited states. Table 1 presents the 2c-TDDFT calculated lowest-energy excitations compared to CASPT2 and LR-CCSD calculations with perturbative spin-orbit corrections.

Pure functionals, such as LSDA, GGA (BLYP and PBE) and meta-GGA (TPSS), tend to yield lower excitation energies compared to all other functionals and to the wave function results. The inclusion of Hartree-Fock exchange has a significant effect on the excitation energies. The results obtained with B3LYP and PBE0 are quite similar, while M062X yields substantially higher excitation energies overall, likely owing to its higher percentage of Hartree-Fock exchange (0.54 %, compared to 20 % and 25 % for B3LYP and PBE0, respectively). The M06HF functional has 100 % HF exchange, and gives the highest excitation energies overall. When compared with the published wave function methods, M062X seems to give results that more closely fall within the interval defined by the CASPT2[115] and LR-CCSD[113] excitation energies.

Table 1. Calculated lowest excited state energies (in eV) of the uranyl(VI) cation. cc-pVTZ basis set[117] is used for oxygen and SARC-DKH basis is used for uranium.[118]

LSDA	BLYP	PBE	TPSS	B3LYP	PBE0	M062X	M06HF	CASPT2[115]	LR-CCSD[113]
1.41	1.22	1.18	1.15	1.61	1.63	2.45	3.21	2.38	2.83
1.57	1.40	1.37	1.35	1.78	1.82	2.58	3.21	2.49	2.85
1.99	1.83	1.76	1.67	2.01	1.95	2.64	3.44	2.51	2.96
2.21	2.06	2.00	1.91	2.26	2.22	2.93	3.68	2.77	3.13
2.33	2.15	2.11	2.09	2.51	2.53	3.35	3.70	3.15	3.45
2.43	2.41	2.37	2.30	2.68	2.64	3.39	3.93	3.26	3.60
2.47	2.42	2.45	2.56	2.92	2.99	3.55	4.10	3.61	4.01
2.57	2.46	2.50	2.56	3.31	3.53	4.00	4.22	3.88	4.30

4 Conclusions and Perspectives

In this work, we presented a two-component non-collinear density functional formalism, which also includes relativistic effects such as spin-orbit coupling using the X2C method,

for the evaluation of excited states. Notably, a similar approach can also be used to assess the stability of the ground-state with respect to any general perturbation. We employ a set of auxiliary variables that take the mixed-spin components of the non-collinear density into account when computing the exchange-correlation part of the energy. An AO direct algorithm is presented in this work that also takes advantages of spin-blocked symmetry of the non-collinear density and transition density.

This non-collinear linear-response formalism requires the functional second derivatives with respect to the non-collinear density and magnetization components. In regions where the magnetization is close to zero, functional second derivatives may encounter numerical instabilities. These numerical issues were resolved by introducing a new set of auxiliary variables defined only in the small magnetization region, without significantly altering the desirable properties of the non-collinear DFT formalism. This approach extends the applicability of the method to all systems, regardless of the spin multiplicity of the reference state.

With this approach we are able to extend existing GGA, meta-GGA, and hybrid functionals to the regime of non-collinear spin. For functionals beyond the local density approximation, through the use of both the parallel and perpendicular components of the magnetization gradient, the definitions of the auxiliary variables presented are able to correctly give rise to non-zero local torque on the magnetization, while maintaining net zero global torque, as it is expected from the exact functional. Several tests were used to validate existing functionals for non-collinear and relativistic calculations using the presented formalism for excited state energetics and properties.

The inclusion of spin-orbit effects in the ground state variationally and in a linear response treatment of the one-electron excitations opens the door to the description of phenomena such as the intersystem crossing between states of different spin-multiplicities. In addition to the transition energy, other excited state properties like transition moments need to be evaluated for both the absorption and emission process (either by fluorescence or phosphorescence).

Future work will also address the energy gradient and Hessian of excited states.

Acknowledgement

The development of the linear response complex two-component DFT method presented in this work is funded by the US Department of Energy (DE-SC0006863). The development of non-Hermitian energy-specific solver for obtaining the eigenfunction of the complex relativistic response function is supported by the US National Science Foundation (CHE-1565520 and CHE-1464497). This work was facilitated though the use of advanced computational, storage, and networking infrastructure provided by the Hyak supercomputer system at the University of Washington. This work is further supported by the U.S. National Science Foundation Graduate Research Fellowship No. DGE-1256082 to J.J.G.

Appendix: Non-collinear exchange-correlation functional derivatives

In this appendix, we present derivations of the exchange-correlation functional derivatives with respect to non-collinear density matrix, including the working equations for the first and second derivative of E_{xc}.

A1. Fundamental variables

In order to allow for non-collinearity, the spin orbitals are expressed as a two-component spinor,

$$\psi_k(\mathbf{x},t) = \begin{pmatrix} \phi_k^{\alpha}(\mathbf{r},t) \\ \phi_k^{\beta}(\mathbf{r},t) \end{pmatrix} \tag{16}$$

where the spatial functions $\{\phi_k^{\alpha}(\mathbf{r},t)\}$, $\{\phi_k^{\beta}(\mathbf{r},t)\}$ are expanded in terms of a common set of real atomic orbital (AO) basis functions $\{\chi_\mu(\mathbf{r})\}$

$$\phi_k^{\alpha}(\mathbf{r},t) = \sum_{\mu} C_{\mu k}^{\alpha}(t)\chi_\mu(\mathbf{r}) \tag{17}$$

$$\phi_k^{\beta}(\mathbf{r},t) = \sum_{\mu} C_{\mu k}^{\beta}(t)\chi_\mu(\mathbf{r}) \tag{18}$$

where the expansion coefficients C's may take complex values.

With the definition of the two-component spinor, the density matrix comprises four independent spin-blocks ($\alpha\alpha$, $\alpha\beta$, $\beta\alpha$, and $\beta\beta$),

$$\mathbf{P} = \begin{pmatrix} \mathbf{P}^{\alpha\alpha} & \mathbf{P}^{\alpha\beta} \\ \mathbf{P}^{\beta\alpha} & \mathbf{P}^{\beta\beta} \end{pmatrix} \tag{19}$$

$$P_{\mu\nu}^{\tau\tau'}(t) = \sum_{i\in\mathrm{occ}} C_{\mu i}^{\tau}(t) C_{\nu i}^{\tau'*}(t), \qquad \tau,\tau' = \alpha,\beta \tag{20}$$

which can be further expanded into their real and imaginary (R/I) and then symmetric/antisymmetric (S/A) components,

$$\mathbf{P} = \begin{pmatrix} \mathbf{P}^{\alpha\alpha\mathrm{RS}} + i\mathbf{P}^{\alpha\alpha\mathrm{IA}} & \mathbf{P}^{\alpha\beta\mathrm{RS}} + \mathbf{P}^{\alpha\beta\mathrm{RA}} + i(\mathbf{P}^{\alpha\beta\mathrm{IS}} + \mathbf{P}^{\alpha\beta\mathrm{IA}}) \\ \mathbf{P}^{\alpha\beta\mathrm{RS}} - \mathbf{P}^{\alpha\beta\mathrm{RA}} - i(\mathbf{P}^{\alpha\beta\mathrm{IS}} - \mathbf{P}^{\alpha\beta\mathrm{IA}}) & \mathbf{P}^{\beta\beta\mathrm{RS}} + i\mathbf{P}^{\beta\beta\mathrm{IA}} \end{pmatrix} \tag{21}$$

Note certain symmetry blocks of the density matrix vanish due to the Hermiticity of $\mathbf{P}$ (e.g. $\mathbf{P}^{\alpha\alpha\mathrm{IS}} = \mathbf{P}^{\beta\beta\mathrm{IS}} = \mathbf{0}$). Using the set of variables defined in Eq. (8) no contribution can arise from the antisymmetric AO density components, since such variables only involve symmetric combination of AO basis functions. The antisymmetric matrices would be involved if the E_{xc} depended on the current densities, but we do not consider this extension here. Nevertheless, the antisymmetric AO densities do contribute to the Hartree-Fock exchange in hybrid functionals.[31] Following the notation of Eq. (21) and dropping the superscript S in the components, the symmetric part of the two-component ground state density can be written as

$$\begin{pmatrix} \mathbf{P}^{\alpha\alpha\mathrm{R}} & \mathbf{P}^{\alpha\beta\mathrm{R}} + i\mathbf{P}^{\alpha\beta\mathrm{I}} \\ \mathbf{P}^{\alpha\beta\mathrm{R}} - i\mathbf{P}^{\alpha\beta\mathrm{I}} & \mathbf{P}^{\beta\beta\mathrm{R}} \end{pmatrix} \tag{22}$$

Upon contraction of the density matrix with the AO basis functions, the scalar total charge density $n(\mathbf{r})$ and magnetization density vector $\mathbf{m}(\mathbf{r})$ can be constructed,[31]

$$n(\mathbf{r}) = \sum_{i\in\mathrm{occ}} \psi_i^\dagger(\mathbf{r})\psi_i(\mathbf{r}) = \sum_{\mu\nu}(P_{\mu\nu}^{\alpha\alpha\mathrm{R}} + P_{\mu\nu}^{\beta\beta\mathrm{R}})\chi_\mu(\mathbf{r})\chi_\nu(\mathbf{r}) \tag{23}$$

$$m_x(\mathbf{r}) = \sum_{i\in\mathrm{occ}} \psi_i^\dagger(\mathbf{r})\sigma_x\psi_i(\mathbf{r}) = 2\sum_{\mu\nu} P_{\mu\nu}^{\alpha\beta\mathrm{R}}\chi_\mu(\mathbf{r})\chi_\nu(\mathbf{r}) \tag{24}$$

$$m_y(\mathbf{r}) = \sum_{i\in\mathrm{occ}} \psi_i^\dagger(\mathbf{r})\sigma_y\psi_i(\mathbf{r}) = -2\sum_{\mu\nu} P_{\mu\nu}^{\alpha\beta\mathrm{I}}\chi_\mu(\mathbf{r})\chi_\nu(\mathbf{r}) \tag{25}$$

$$m_z(\mathbf{r}) = \sum_{i\in\mathrm{occ}} \psi_i^\dagger(\mathbf{r})\sigma_z\psi_i(\mathbf{r}) = \sum_{\mu\nu}(P_{\mu\nu}^{\alpha\alpha\mathrm{R}} - P_{\mu\nu}^{\beta\beta\mathrm{R}})\chi_\mu(\mathbf{r})\chi_\nu(\mathbf{r}) \tag{26}$$

where σ_k are Pauli matrices.

$$\sigma_x = \begin{pmatrix} 0 & 1 \\ 1 & 0 \end{pmatrix}, \quad \sigma_y = \begin{pmatrix} 0 & -i \\ i & 0 \end{pmatrix}, \quad \sigma_z = \begin{pmatrix} 1 & 0 \\ 0 & -1 \end{pmatrix} \tag{27}$$

A2. Functional variables

For GGA, the exchange-correlation functional has the general form

$$E_{xc} = \int f(n^+, n^-, \gamma^{++}, \gamma^{--}, \gamma^{+-}, \tau^+, \tau^-) d\mathbf{r} \tag{28}$$

for meta-GGA,

$$E_{xc} = \int f(n^+, n^-, \gamma^{++}, \gamma^{--}, \gamma^{+-}, \tau^+, \tau^-, \nabla^2\rho^+, \nabla^2\rho^-) d\mathbf{r} \tag{29}$$

where f is a function of auxiliary variables $\{U_i\}$

$$\{U_i\} = \left\{ n^+ \quad n^- \quad \gamma^{++} \quad \gamma^{--} \quad \gamma^{+-} \quad \tau^+ \quad \tau^- \quad \nabla^2\rho^+ \quad \nabla^2\rho^- \right\} \tag{30}$$

$\{U_i\}$ are defined as functions of density variables $\{V_i\}$ in Eq. (8),

$$\{V_i\} = \left\{ \begin{array}{cccccccc} n & m_x & m_y & m_z & \tau & u_x & u_y & u_z \\ \nabla n & \nabla m_x & \nabla m_y & \nabla m_z & \nabla^2 n & \nabla^2 m_x & \nabla^2 m_y & \nabla^2 m_z \end{array} \right\} \tag{31}$$

$n(\mathbf{r})$ and $\mathbf{m}(\mathbf{r})$ are defined in Eqs. (23) to (26). Scalar $\tau(\mathbf{r})$ and vector $\mathbf{u}(\mathbf{r})$ are

$$\tau(\mathbf{r}) = \frac{1}{2}\sum_{i\in\mathrm{occ}}[\boldsymbol{\nabla}\psi_i(\mathbf{r})]^\dagger\cdot\boldsymbol{\nabla}\psi_i(\mathbf{r}) = \frac{1}{2}\sum_{\mu\nu}(P^{\alpha\alpha\mathrm{R}}_{\mu\nu}+P^{\beta\beta\mathrm{R}}_{\mu\nu})\,\boldsymbol{\nabla}\chi_\mu(\mathbf{r})\cdot\boldsymbol{\nabla}\chi_\nu(\mathbf{r}) \tag{32}$$

$$u_x(\mathbf{r}) = \frac{1}{2}\sum_{i\in\mathrm{occ}}[\boldsymbol{\nabla}\psi_i(\mathbf{r})]^\dagger\cdot\sigma_x\boldsymbol{\nabla}\psi_i(\mathbf{r}) = \sum_{\mu\nu}P^{\alpha\beta\mathrm{R}}_{\mu\nu}\boldsymbol{\nabla}\chi_\mu(\mathbf{r})\cdot\boldsymbol{\nabla}\chi_\nu(\mathbf{r}) \tag{33}$$

$$u_y(\mathbf{r}) = \frac{1}{2}\sum_{i\in\mathrm{occ}}[\boldsymbol{\nabla}\psi_i(\mathbf{r})]^\dagger\cdot\sigma_y\boldsymbol{\nabla}\psi_i(\mathbf{r}) = -\sum_{\mu\nu}P^{\alpha\beta\mathrm{I}}_{\mu\nu}\boldsymbol{\nabla}\chi_\mu(\mathbf{r})\cdot\boldsymbol{\nabla}\chi_\nu(\mathbf{r}) \tag{34}$$

$$u_z(\mathbf{r}) = \frac{1}{2}\sum_{i\in\mathrm{occ}}[\boldsymbol{\nabla}\psi_i(\mathbf{r})]^\dagger\cdot\sigma_z\boldsymbol{\nabla}\psi_i(\mathbf{r}) = \frac{1}{2}\sum_{\mu\nu}(P^{\alpha\alpha\mathrm{R}}_{\mu\nu}-P^{\beta\beta\mathrm{R}}_{\mu\nu})\boldsymbol{\nabla}\chi_\mu(\mathbf{r})\cdot\boldsymbol{\nabla}\chi_\nu(\mathbf{r}) \tag{35}$$

The gradient and laplacian of $n(\mathbf{r})$ and $\mathbf{m}(\mathbf{r})$ are defined as

$$\boldsymbol{\nabla}n(\mathbf{r}) = \sum_{\mu\nu}(P^{\alpha\alpha\mathrm{R}}_{\mu\nu}+P^{\beta\beta\mathrm{R}}_{\mu\nu})\boldsymbol{\nabla}(\chi_\mu(\mathbf{r})\chi_\nu(\mathbf{r})) \tag{36}$$

$$\boldsymbol{\nabla}m_z(\mathbf{r}) = \sum_{\mu\nu}(P^{\alpha\alpha\mathrm{R}}_{\mu\nu}-P^{\beta\beta\mathrm{R}}_{\mu\nu})\boldsymbol{\nabla}(\chi_\mu(\mathbf{r})\chi_\nu(\mathbf{r})) \tag{37}$$

$$\boldsymbol{\nabla}m_x(\mathbf{r}) = 2\sum_{\mu\nu}P^{\alpha\beta\mathrm{R}}_{\mu\nu}\boldsymbol{\nabla}(\chi_\mu(\mathbf{r})\chi_\nu(\mathbf{r})) \tag{38}$$

$$\boldsymbol{\nabla}m_y(\mathbf{r}) = -2\sum_{\mu\nu}P^{\alpha\beta\mathrm{I}}_{\mu\nu}\boldsymbol{\nabla}(\chi_\mu(\mathbf{r})\chi_\nu(\mathbf{r})) \tag{39}$$

$$\nabla^2 n(\mathbf{r}) = \sum_{\mu\nu} (P_{\mu\nu}^{\alpha\alpha\mathrm{R}} + P_{\mu\nu}^{\beta\beta\mathrm{R}}) \nabla^2 (\chi_\mu(\mathbf{r}) \chi_\nu(\mathbf{r})) \tag{40}$$

$$\nabla^2 m_z(\mathbf{r}) = \sum_{\mu\nu} (P_{\mu\nu}^{\alpha\alpha\mathrm{R}} - P_{\mu\nu}^{\beta\beta\mathrm{R}}) \nabla^2 (\chi_\mu(\mathbf{r}) \chi_\nu(\mathbf{r})) \tag{41}$$

$$\nabla^2 m_x(\mathbf{r}) = 2 \sum_{\mu\nu} P_{\mu\nu}^{\alpha\beta\mathrm{R}} \nabla^2 (\chi_\mu(\mathbf{r}) \chi_\nu(\mathbf{r})) \tag{42}$$

$$\nabla^2 m_y(\mathbf{r}) = -2 \sum_{\mu\nu} P_{\mu\nu}^{\alpha\beta\mathrm{I}} \nabla^2 (\chi_\mu(\mathbf{r}) \chi_\nu(\mathbf{r})) \tag{43}$$

These density variables $\{V_i\}$ are linear in density matrix blocks, and the functional derivatives can be obtained via the chain rule.

A3. Functional first derivatives

The first derivative of E_{xc} with respect to the density matrix elements can be calculated via the chain rule,

$$(F_{xc}^{NC})_{\mu\nu} = \frac{\partial E_{xc}^{NC}}{\partial P_{\nu\mu}} = \sum_{ij} \int \frac{\partial f(\{U_i(\mathbf{r})\})}{\partial U_i(\mathbf{r})} \frac{\partial U_i(\mathbf{r})}{\partial V_j(\mathbf{r})} \frac{\partial V_j(\mathbf{r})}{\partial P_{\nu\mu}} d\mathbf{r} \tag{44}$$

While $\frac{\partial f}{\partial U_i}$ is the same as collinear case, the Jacobians $\frac{\partial U_i}{\partial V_j}$ are different than those in the collinear case. The Jacobian is sparse, and the non-zero elements are listed below. In the following equations, α, β are used to label spin index, and i, j for cartesian index x, y, z. The following equations use the Einstein summation convention.

$n^+(n, m_\alpha)$:

$$\frac{\partial n^+}{\partial n} = \frac{1}{2} \tag{45}$$

$$\frac{\partial n^+}{\partial m_\alpha} = \frac{1}{2} \frac{m_\alpha}{\sqrt{\mathbf{m} \circ \mathbf{m}}} \tag{46}$$

$n^-(n, m_\alpha)$:

$$\frac{\partial n^-}{\partial n} = \frac{1}{2} \tag{47}$$

$$\frac{\partial n^-}{\partial m_\alpha} = -\frac{1}{2}\frac{m_\alpha}{\sqrt{\mathbf{m} \circ \mathbf{m}}} \tag{48}$$

$\gamma^{++}(\partial_i n, \partial_i m_\alpha)$:

$$\frac{\partial \gamma^{++}}{\partial(\partial_i n)} = \frac{1}{2}\partial_i n + \frac{f_{\boldsymbol{\nabla}}}{2}\frac{\partial_i m_\alpha \partial_j m_\alpha \partial_j n}{\sqrt{\boldsymbol{\nabla} n \cdot \boldsymbol{\nabla}\mathbf{m} \circ \boldsymbol{\nabla}\mathbf{m} \cdot \boldsymbol{\nabla} n}} \tag{49}$$

$$\frac{\partial \gamma^{++}}{\partial(\partial_i m_\alpha)} = \frac{1}{2}\partial_i m_\alpha + \frac{f_{\boldsymbol{\nabla}}}{2}\frac{\partial_i n \partial_j m_\alpha \partial_j n}{\sqrt{\boldsymbol{\nabla} n \cdot \boldsymbol{\nabla}\mathbf{m} \circ \boldsymbol{\nabla}\mathbf{m} \cdot \boldsymbol{\nabla} n}} \tag{50}$$

$\gamma^{--}(\partial_i n, \partial_i m_\alpha)$:

$$\frac{\partial \gamma^{--}}{\partial(\partial_i n)} = \frac{1}{2}\partial_i n - \frac{f_{\boldsymbol{\nabla}}}{2}\frac{\partial_i m_\alpha \partial_j m_\alpha \partial_j n}{\sqrt{\boldsymbol{\nabla} n \cdot \boldsymbol{\nabla}\mathbf{m} \circ \boldsymbol{\nabla}\mathbf{m} \cdot \boldsymbol{\nabla} n}} \tag{51}$$

$$\frac{\partial \gamma^{--}}{\partial(\partial_i m_\alpha)} = \frac{1}{2}\partial_i m_\alpha - \frac{f_{\boldsymbol{\nabla}}}{2}\frac{\partial_i n \partial_j m_\alpha \partial_j n}{\sqrt{\boldsymbol{\nabla} n \cdot \boldsymbol{\nabla}\mathbf{m} \circ \boldsymbol{\nabla}\mathbf{m} \cdot \boldsymbol{\nabla} n}} \tag{52}$$

$\gamma^{+-}(\partial_i n, \partial_i m_\alpha)$:

$$\frac{\partial \gamma^{+-}}{\partial(\partial_i n)} = \frac{1}{2}\partial_i n \tag{53}$$

$$\frac{\partial \gamma^{+-}}{\partial(\partial_i m_\alpha)} = -\frac{1}{2}\partial_i m_\alpha \tag{54}$$

$\tau^+(\tau, u_\alpha)$:

$$\frac{\partial \tau^+}{\partial \tau} = \frac{1}{2} \tag{55}$$

$$\frac{\partial \tau^+}{\partial u_\alpha} = \frac{f_{\mathbf{u}}}{2}\frac{u_\alpha}{\sqrt{\mathbf{u} \circ \mathbf{u}}} \tag{56}$$

$\tau^-(\tau, u_\alpha)$:

$$\frac{\partial \tau^-}{\partial \tau} = \frac{1}{2} \tag{57}$$

$$\frac{\partial \tau^-}{\partial u_\alpha} = -\frac{f_{\mathbf{u}}}{2} \frac{u_\alpha}{\sqrt{\mathbf{u} \circ \mathbf{u}}} \tag{58}$$

$\nabla^2\rho^+(\nabla^2 n, \nabla^2 m_\alpha)$:

$$\frac{\partial \nabla^2 \rho^+}{\partial \nabla^2 n} = \frac{1}{2} \tag{59}$$

$$\frac{\partial \nabla^2 \rho^+}{\partial \nabla^2 m_\alpha} = \frac{f_{\nabla^2}}{2} \frac{\nabla^2 m_\alpha}{\sqrt{\nabla^2 \mathbf{m} \circ \nabla^2 \mathbf{m}}} \tag{60}$$

$\nabla^2\rho^-(\nabla^2 n, \nabla^2 m_\alpha)$:

$$\frac{\partial \nabla^2 \rho^-}{\partial \nabla^2 n} = \frac{1}{2} \tag{61}$$

$$\frac{\partial \nabla^2 \rho^-}{\partial \nabla^2 m_\alpha} = -\frac{f_{\nabla^2}}{2} \frac{\nabla^2 m_\alpha}{\sqrt{\nabla^2 \mathbf{m} \circ \nabla^2 \mathbf{m}}} \tag{62}$$

A4. Functional second derivatives

Second derivative of E_{xc} with respect to the density matrix elements is required to assemble the **A** and **B** matrix in linear response and stability calculation. Functional second derivatives can be derived by applying a second chain rule,

$$\frac{\partial^2 E_{xc}}{\partial P_{\mu\nu} \partial P_{\kappa\lambda}} = \sum_{ijkl} \int \left(\frac{\partial^2 f}{\partial U_i \partial U_l} \frac{\partial U_i}{\partial V_j} \frac{\partial U_l}{\partial V_k} + \frac{\partial f}{\partial U_i} \frac{\partial^2 U_i}{\partial V_j \partial V_k} \right) \frac{\partial V_j}{\partial P_{\mu\nu}} \frac{\partial V_k}{\partial P_{\kappa\lambda}} d\mathbf{r} \tag{63}$$

Non-zero elements of second derivatives of $\{U_i\}$ with respect to $\{V_i\}$ are listed below.

n^+:

$$\frac{\partial^2 n^+}{\partial m_\alpha \partial m_\beta} = \frac{1}{2} \left(\frac{\delta_{\alpha\beta}}{\sqrt{\mathbf{m} \circ \mathbf{m}}} - \frac{m_\alpha m_\beta}{(\sqrt{\mathbf{m} \circ \mathbf{m}})^3} \right) \tag{64}$$

n^-:

$$\frac{\partial^2 n^-}{\partial m_\alpha \partial m_\beta} = -\frac{1}{2}\left(\frac{\delta_{\alpha\beta}}{\sqrt{\mathbf{m}\circ\mathbf{m}}} - \frac{m_\alpha m_\beta}{(\sqrt{\mathbf{m}\circ\mathbf{m}})^3}\right) \tag{65}$$

γ^{++}

$$\frac{\partial \gamma^{++}}{\partial(\partial_i n)\partial(\partial_j n)} = \frac{1}{2}\delta_{ij} + \frac{f_{\boldsymbol{\nabla}}}{2}\left(\frac{\partial_i m_\alpha \partial_j m_\alpha}{\sqrt{\boldsymbol{\nabla} n\cdot\boldsymbol{\nabla}\mathbf{m}\circ\boldsymbol{\nabla}\mathbf{m}\cdot\boldsymbol{\nabla} n}} - \frac{\partial_i m_\alpha \partial_k m_\alpha \partial_k n \partial_l n \partial_l m_\beta \partial_j m_\beta}{(\sqrt{\boldsymbol{\nabla} n\cdot\boldsymbol{\nabla}\mathbf{m}\circ\boldsymbol{\nabla}\mathbf{m}\cdot\boldsymbol{\nabla} n})^3}\right) \tag{66}$$

$$\frac{\partial^2 \gamma^{++}}{\partial(\partial_i n)\partial(\partial_j m_\alpha)} = \frac{f_{\boldsymbol{\nabla}}}{2}\left(\frac{\partial_i m_\alpha \partial_j n + \delta_{ij}\partial_k m_\alpha \partial_k n}{\sqrt{\boldsymbol{\nabla} n\cdot\boldsymbol{\nabla}\mathbf{m}\circ\boldsymbol{\nabla}\mathbf{m}\cdot\boldsymbol{\nabla} n}} - \frac{\partial_i m_\beta \partial_k m_\beta \partial_k n \partial_j n \partial_l m_\alpha \partial_l n}{(\sqrt{\boldsymbol{\nabla} n\cdot\boldsymbol{\nabla}\mathbf{m}\circ\boldsymbol{\nabla}\mathbf{m}\cdot\boldsymbol{\nabla} n})^3}\right) \tag{67}$$

$$\frac{\partial^2 \gamma^{++}}{\partial(\partial_i m_\alpha)\partial(\partial_j m_\beta)} = \frac{\delta_{ij}\delta_{\alpha\beta}}{2} + \frac{f_{\boldsymbol{\nabla}}}{2}\left(\frac{\delta_{\alpha\beta}\partial_i n \partial_j n}{\sqrt{\boldsymbol{\nabla} n\cdot\boldsymbol{\nabla}\mathbf{m}\circ\boldsymbol{\nabla}\mathbf{m}\cdot\boldsymbol{\nabla} n}} - \frac{\partial_i n \partial_k m_\alpha \partial_k n \partial_l n \partial_l m_\beta \partial_j n}{(\sqrt{\boldsymbol{\nabla} n\cdot\boldsymbol{\nabla}\mathbf{m}\circ\boldsymbol{\nabla}\mathbf{m}\cdot\boldsymbol{\nabla} n})^3}\right) \tag{68}$$

γ^{--}

$$\frac{\partial \gamma^{--}}{\partial(\partial_i n)\partial(\partial_j n)} = \frac{1}{2}\delta_{ij} - \frac{f_{\boldsymbol{\nabla}}}{2}\left(\frac{\partial_i m_\alpha \partial_j m_\alpha}{\sqrt{\boldsymbol{\nabla} n\cdot\boldsymbol{\nabla}\mathbf{m}\circ\boldsymbol{\nabla}\mathbf{m}\cdot\boldsymbol{\nabla} n}} - \frac{\partial_i m_\alpha \partial_k m_\alpha \partial_k n \partial_l n \partial_l m_\beta \partial_j m_\beta}{(\sqrt{\boldsymbol{\nabla} n\cdot\boldsymbol{\nabla}\mathbf{m}\circ\boldsymbol{\nabla}\mathbf{m}\cdot\boldsymbol{\nabla} n})^3}\right) \tag{69}$$

$$\frac{\partial^2 \gamma^{--}}{\partial(\partial_i n)\partial(\partial_j m_\alpha)} = -\frac{f_{\boldsymbol{\nabla}}}{2}\left(\frac{\partial_i m_\alpha \partial_j n + \delta_{ij}\partial_k m_\alpha \partial_k n}{\sqrt{\boldsymbol{\nabla} n\cdot\boldsymbol{\nabla}\mathbf{m}\circ\boldsymbol{\nabla}\mathbf{m}\cdot\boldsymbol{\nabla} n}} - \frac{\partial_i m_\beta \partial_k m_\beta \partial_k n \partial_j n \partial_l m_\alpha \partial_l n}{(\sqrt{\boldsymbol{\nabla} n\cdot\boldsymbol{\nabla}\mathbf{m}\circ\boldsymbol{\nabla}\mathbf{m}\cdot\boldsymbol{\nabla} n})^3}\right) \tag{70}$$

$$\frac{\partial^2 \gamma^{--}}{\partial(\partial_i m_\alpha)\partial(\partial_j m_\beta)} = \frac{\delta_{ij}\delta_{\alpha\beta}}{2} - \frac{f_{\boldsymbol{\nabla}}}{2}\left(\frac{\delta_{\alpha\beta}\partial_i n \partial_j n}{\sqrt{\boldsymbol{\nabla} n\cdot\boldsymbol{\nabla}\mathbf{m}\circ\boldsymbol{\nabla}\mathbf{m}\cdot\boldsymbol{\nabla} n}} - \frac{\partial_i n \partial_k m_\alpha \partial_k n \partial_l n \partial_l m_\beta \partial_j n}{(\sqrt{\boldsymbol{\nabla} n\cdot\boldsymbol{\nabla}\mathbf{m}\circ\boldsymbol{\nabla}\mathbf{m}\cdot\boldsymbol{\nabla} n})^3}\right) \tag{71}$$

γ^{+-}

$$\frac{\partial^2 \gamma^{+-}}{\partial(\partial_i n)\partial(\partial_j n)} = \frac{1}{2}\delta_{ij} \tag{72}$$

$$\frac{\partial^2 \gamma^{+-}}{\partial(\partial_i m_\alpha)\partial(\partial_j m_\beta)} = -\frac{1}{2}\delta_{ij}\delta_{\alpha\beta} \tag{73}$$

$\nabla^2\rho^+$:

$$\frac{\partial(\nabla^2\rho^+)}{\partial(\nabla^2 m_\alpha)\partial(\nabla^2 m_\beta)} = \frac{f_{\nabla^2}}{2}\left(\frac{\delta_{\alpha\beta}}{\sqrt{\nabla^2\mathbf{m}\circ\nabla^2\mathbf{m}}} - \frac{\nabla^2 m_\alpha \nabla^2 m_\beta}{(\sqrt{\nabla^2\mathbf{m}\circ\nabla^2\mathbf{m}})^3}\right) \tag{74}$$

$\nabla^2\rho^-$:

$$\frac{\partial(\nabla^2\rho^-)}{\partial(\nabla^2 m_\alpha)\partial(\nabla^2 m_\beta)} = -\frac{f_{\nabla^2}}{2}\left(\frac{\delta_{\alpha\beta}}{\sqrt{\nabla^2\mathbf{m}\circ\nabla^2\mathbf{m}}} - \frac{\nabla^2 m_\alpha \nabla^2 m_\beta}{(\sqrt{\nabla^2\mathbf{m}\circ\nabla^2\mathbf{m}})^3}\right) \tag{75}$$

A5. Derivatives with respect to non-collinear density matrix

Derivatives of density variables with respect to the non-collinear density matrix, $\frac{\partial V_i}{\partial \mathbf{P}^{\tau\tau'}}$, are needed in the functional first (Eq. (44)) and second (Eq. (63)) derivative evaluations before they can be contracted with the ground state density matrix or the transition density matrix. Using the expression for the non-collinear density matrix in Eq. (22), the general expression for spin-blocked density derivatives can be written as,

$$\frac{\partial}{\partial \mathbf{P}} = \begin{pmatrix} \frac{\partial}{\partial \mathbf{P}^{\alpha\alpha\mathrm{R}}} & \frac{1}{2}\frac{\partial}{\partial \mathbf{P}^{\alpha\beta\mathrm{R}}} - \frac{i}{2}\frac{\partial}{\partial \mathbf{P}^{\alpha\beta\mathrm{I}}} \\ \frac{1}{2}\frac{\partial}{\partial \mathbf{P}^{\alpha\beta\mathrm{R}}} + \frac{i}{2}\frac{\partial}{\partial \mathbf{P}^{\alpha\beta\mathrm{I}}} & \frac{\partial}{\partial \mathbf{P}^{\beta\beta\mathrm{R}}} \end{pmatrix} \tag{76}$$

Since $\{V_i\}$ are linear in density matrix elements, their derivatives can be easily evaluated using Eq. (76) given the expressions defined in Eqs. (23) to (26) and Eqs. (32) to (35).

A6. Direct contraction of functional second derivatives with non-collinear transition density

The fundamental operation at the core of the iterative solution of Eq. (11) is a matrix-vector product that amounts to contracting the functional second derivatives (Eq. (63)) on the right with a trial two-component non-Hermitian non-collinear transition density $\mathbf{T}$. In order to take advantage of the symmetry of the functional second derivatives with respect to the

non-collinear density matrix (Eq. (76)), the symmetric part of the non-collinear transition density $\mathbf{T}$ in AO basis are separated into spin-blocked ($\alpha\alpha$, $\alpha\beta$, $\beta\alpha$, or $\beta\beta$) real/imaginary (R/I) components:

$$\begin{pmatrix} \mathbf{T}^{\alpha\alpha\mathrm{R}} + i\,\mathbf{T}^{\alpha\alpha\mathrm{I}} & \mathbf{T}^{\alpha\beta\mathrm{R}} + i\,\mathbf{T}^{\alpha\beta\mathrm{I}} \\ \mathbf{T}^{\beta\alpha\mathrm{R}} + i\,\mathbf{T}^{\beta\alpha\mathrm{I}} & \mathbf{T}^{\beta\beta\mathrm{R}} + i\,\mathbf{T}^{\beta\beta\mathrm{I}} \end{pmatrix} \tag{77}$$

with its Hermitian and anti-Hermitian components given by:

$$\mathbf{T}^{\mathrm{H}} = \begin{pmatrix} \mathbf{T}^{\alpha\alpha\mathrm{R}} & \frac{1}{2}\big(\mathbf{T}^{\alpha\beta\mathrm{R}} + \mathbf{T}^{\beta\alpha\mathrm{R}}\big) + \frac{i}{2}\big(\mathbf{T}^{\alpha\beta\mathrm{I}} - \mathbf{T}^{\beta\alpha\mathrm{I}}\big) \\ \frac{1}{2}\big(\mathbf{T}^{\beta\alpha\mathrm{R}} + \mathbf{T}^{\alpha\beta\mathrm{R}}\big) + \frac{i}{2}\big(\mathbf{T}^{\beta\alpha\mathrm{I}} - \mathbf{T}^{\alpha\beta\mathrm{I}}\big) & \mathbf{T}^{\beta\beta\mathrm{R}} \end{pmatrix}$$

$$\mathbf{T}^{\mathrm{AH}} = i \begin{pmatrix} \mathbf{T}^{\alpha\alpha\mathrm{I}} & \frac{1}{2}\big(\mathbf{T}^{\alpha\beta\mathrm{I}} + \mathbf{T}^{\beta\alpha\mathrm{I}}\big) - \frac{i}{2}\big(\mathbf{T}^{\alpha\beta\mathrm{R}} - \mathbf{T}^{\beta\alpha\mathrm{R}}\big) \\ \frac{1}{2}\big(\mathbf{T}^{\beta\alpha\mathrm{I}} + \mathbf{T}^{\alpha\beta\mathrm{I}}\big) - \frac{i}{2}\big(\mathbf{T}^{\beta\alpha\mathrm{R}} - \mathbf{T}^{\alpha\beta\mathrm{R}}\big) & \mathbf{T}^{\beta\beta\mathrm{I}} \end{pmatrix}$$

Since the *xc* kernel originates from a Hermitian ground state, only eight contraction steps give rise to non-zero contributions,

$$\begin{aligned} &\frac{\partial^2 E_{\mathrm{xc}}}{\partial\mathbf{P}\partial\mathbf{P}^{\alpha\alpha\mathrm{R}}}\,\mathbf{T}^{\alpha\alpha\mathrm{R}} && \frac{\partial^2 E_{\mathrm{xc}}}{\partial\mathbf{P}\partial\mathbf{P}^{\alpha\beta\mathrm{R}}}\,\frac{1}{2}\big(\mathbf{T}^{\alpha\beta\mathrm{R}} + \mathbf{T}^{\beta\alpha\mathrm{R}}\big) \\ &\frac{\partial^2 E_{\mathrm{xc}}}{\partial\mathbf{P}\partial\mathbf{P}^{\beta\beta\mathrm{R}}}\,\mathbf{T}^{\beta\beta\mathrm{R}} && \frac{\partial^2 E_{\mathrm{xc}}}{\partial\mathbf{P}\partial\mathbf{P}^{\alpha\beta\mathrm{I}}}\,\frac{1}{2}\big(\mathbf{T}^{\alpha\beta\mathrm{I}} - \mathbf{T}^{\beta\alpha\mathrm{I}}\big) \\ i\,&\frac{\partial^2 E_{\mathrm{xc}}}{\partial\mathbf{P}\partial\mathbf{P}^{\alpha\alpha\mathrm{R}}}\,\mathbf{T}^{\alpha\alpha\mathrm{I}} && i\,\frac{\partial^2 E_{\mathrm{xc}}}{\partial\mathbf{P}\partial\mathbf{P}^{\alpha\beta\mathrm{R}}}\,\frac{1}{2}\big(\mathbf{T}^{\alpha\beta\mathrm{I}} + \mathbf{T}^{\beta\alpha\mathrm{I}}\big) \\ i\,&\frac{\partial^2 E_{\mathrm{xc}}}{\partial\mathbf{P}\partial\mathbf{P}^{\beta\beta\mathrm{R}}}\,\mathbf{T}^{\beta\beta\mathrm{I}} && i\,\frac{\partial^2 E_{\mathrm{xc}}}{\partial\mathbf{P}\partial\mathbf{P}^{\alpha\beta\mathrm{I}}}\,\frac{-1}{2}\big(\mathbf{T}^{\alpha\beta\mathrm{R}} - \mathbf{T}^{\beta\alpha\mathrm{R}}\big) \end{aligned}$$

References

(1) Sanvito, S. Molecular Spintronics. *Chem. Soc. Rev.* **2011**, *40*, 3336–3355.

(2) Rocha, A. R.; Garcia-Suarez, V. M.; Bailey, S. W.; Lambert, C. J.; Ferrer, J.; Sanvito, S. Towards Molecular Spintronics. *Nat. Mater.* **2005**, *4*, 335–339.

(3) Moodera, J. S.; Santos, T. S.; Nagahama, T. The Phenomena of Spin-filter Tunnelling. *J. Phys.–Condens. Mat.* **2007**, *19*, 165202.

(4) Ovchinnikov, I. V.; Neuhauser, D. Spintronics birefringence with an extended molecular loop-wire or spiral coupling. *J. Chem. Phys.* **2005**, *123*, 204714.

(5) Dyall, K. G.; Fægri, Jr., K. *Introduction to Relativistic Quantum Chemistry*; Oxford University Press: Oxford, U.K., 2007.

(6) Reiher, M.; Wolf, A. *Relativistic Quantum Chemistry*, 2nd ed.; Wiley-VCH, 2015.

(7) Pyykkö, P. Relativistic Effects in Chemistry: More Common Than You Thought. *Annu. Rev. Phys. Chem.* **2012**, *63*, 45–64.

(8) Cheong, S.-W.; Mostovoy, M. Multiferroics: a magnetic twist for ferroelectricity. *Nat. Mater.* **2007**, *6*, 13–20.

(9) Dzyaloshinsky, I. A thermodynamic theory of "weak" ferromagnetism of antiferromagnetics. *J. Phys. Chem. Solids* **1958**, *4*, 241–255.

(10) Moriya, T. Anisotropic Superexchange Interaction and Weak Ferromagnetism. *Phys. Rev.* **1960**, *120*, 91–98.

(11) Eich, F. G.; Gross, E. K. U. Transverse Spin-Gradient Functional for Noncollinear Spin-Density-Functional Theory. *Phys. Rev. Lett.* **2013**, *111*, 156401.

(12) Anton, J.; Fricke, B.; Engel, E. Noncollinear and collinear relativistic density-functional program for electric and magnetic properties of molecules. *Phys. Rev. A* **2004**, *69*, 012505.

(13) Devarajan, A.; Gaenko, A.; Autschbach, J. Two-Component Relativistic Density Functional Method for Computing Nonsingular Complex Linear Response of Molecules Based on the Zeroth Order Regular Approximation. *J. Chem. Phys.* **2009**, *130*, 194102.

(14) Wang, F.; Ziegler, T. Time-Dependent Density Functional Theory Based on a Noncollinear Formulation of the Exchange-Correlation Potential. *J. Chem. Phys.* **2004**, *121*, 12191–12196.

(15) Wang, F.; Ziegler, T.; van Lenthe, E.; van Gisbergen, S.; Baerends, E. J. The Calculation of Excitation Energies Based on the Relativistic Two-Component Zeroth-Order Regular Approximation and Time-Dependent Density-Functional with Full Use of Symmetry. *J. Chem. Phys.* **2005**, *122*, 204103.

(16) Casarin, M.; Finetti, P.; Vittadini, A.; Wang, F.; Ziegler, T. Spin-Orbit Relativistic Time-Dependent Density Functional Calculations of the Metal and Ligand Pre-Edge XAS Intensities of Organotitanium Complexes: $TiCl_4$, Ti(η^5-C_5H_5)Cl_3, and Ti(η^5-C_5H_5)$_2Cl_2$. *J. Phys. Chem. A* **2007**, *111*, 5270–5279.

(17) Kün, M.; Weigend, F. Implementation of Two-Component Time-Dependent Density Functional Theory in TURBOMOLE. *J. Chem. Theory Comput.* **2013**, *9*, 5341–5348.

(18) van Wüllen, C. Spin Densities in Two-Component Relativistic Density Functional Calculations: Noncollinear versus Collinear Approach. *J. Comput. Chem.* **2002**, *23*, 779–785.

(19) Peralta, J. E.; Scuseria, G. E.; Frisch, M. J. Noncollinear magnetism in density functional calculations. *Phys. Rev. B* **2007**, *75*, 125119.

(20) Scalmani, G.; Frisch, M. J. A New Approach to Noncollinear Spin Density Functional Theory beyond the Local Density Approximation. *J. Chem. Theory Comput.* **2012**, *8*, 2193–2196.

(21) Bulik, I. W.; Scalmani, G.; Frisch, M. J.; Scuseria, G. E. Noncollinear Density Functional Theory Having Proper Invariance and Local Torque Properties. *Phys. Rev. B* **2013**, *87*, 035117.

(22) Bast, R.; Jensen, H. J. A.; Saue, T. Relativistic Adiabatic Time-Dependent Density Functional Theory Using Hybrid Functionals and Noncollinear Spin Magnetization. *Int. J. Quant. Chem.* **2009**, *109*, 2091–2112.

(23) Gao, J.; ; Liu, W.; Song, B.; Liu, C. Time-Dependent Four-Component Relativistic Density Functional Theory for Excitation Energies. *J. Chem. Phys.* **2004**, *121*, 6658–6666.

(24) Liu, W.; Peng, D. Infinite-Order Quasirelativistic Density Functional Method Based on the Exact Matrix Quasirelativistic Theory. *J. Chem. Phys.* **2006**, *125*, 044102.

(25) Kutzelnigg, W.; Liu, W. Quasirelativistic Theory Equivalent to Fully Relativistic Theory. *J. Chem. Phys.* **2005**, *123*, 241102.

(26) Wang, F.; Liu, W. Comparison of Different Polarization Schemes in Open-shell Relativistic Density Functional Calculations. *J. Chin. Chem. Soc.* **2003**, *50*, 597–606.

(27) Gao, J.; Zou, W.; Liu, W.; Xiao, Y.; Peng, D.; Song, B.; Liu, C. Time-Dependent Four-Component Relativistic Density-Functional Theory for Excitation Energies. II. The Exchange-Correlation Kernel. *J. Chem. Phys.* **2005**, *123*, 054102.

(28) Li, Z.; Suo, B.; Zhang, Y.; Xiao, Y.; Liu, W. Combining Spin-Adapted Open-Shell TD-DFT with SpinOrbit Coupling. *Mol. Phys.* **2013**, *111*, 3741–3755.

(29) Goings, J. J.; Kasper, J. M.; Egidi, F.; Sun, S.; Li, X. Real Time Propagation of the Exact Two Component Time-Dependent Density Functional Theory. *J. Chem. Phys.* **2016**, *145*, 104107.

(30) Ding, F.; Goings, J. J.; Frisch, M. J.; Li, X. Ab Initio Non-Relativistic Spin Dynamics. *J. Chem. Phys.* **2014**, *141*, 214111.

(31) Egidi, F.; Goings, J. J.; Frisch, M. J.; Li, X. Direct Atomic-Orbital-Based Relativistic Two-Component Linear Response Method for Calculating Excited-State Fine Structures. *J. Chem. Theory Comput.* **2016**, *12*, 3711–3718.

(32) Williams-Young, D.; Egidi, F.; Li, X. Relativistic Two-Component Particle–Particle Tamm–Dancoff Approximation. *J. Chem. Theory Comput.* **2016**, 5379–5384.

(33) Hess, B. A. Applicability of the No-Pair Equation with Free-Particle Projection Operators to Atomic and Molecular Structure Calculations. *Phys. Rev. A* **1985**, *32*, 756–763.

(34) Hess, B. A. Relativistic Electronic-Structure Calculations Employing a Two-Component No-Pair Formalism with External-Field Projection Operators. *Phys. Rev. A* **1986**, *33*, 3742–3748.

(35) Peralta, J. E.; Scuseria, G. E. Relativistic All-Electron Two-Component Self-Consistent Density Functional Calculations Including One-Electron Scalar and Spin-Orbit Effects. *J. Chem. Phys.* **2004**, *120*, 5875.

(36) Filatov, M.; Cremer, D. A New Quasi-Relativistic Approach for Density Functional Theory Based on the Normalized Elimination of the Small Component. *Chem. Phys. Lett.* **2002**, *351*, 259–266.

(37) Filatov, M.; Zou, W.; Cremer, D. Spin-Orbit Coupling Calculations with the Two-

Component Normalized Elimination of the Small Component Method. *J. Chem. Phys.* **2013**, *139*, 014106.

(38) Ilias, M.; Saue, T. An Infinite-Order Relativistic Hamiltonian by a Simple One-Step Transformation. *J. Chem. Phys.* **2007**, *126*, 064102.

(39) Saue, T. Relativistic Hamiltonians for Chemistry: A Primer. *ChemPhysChem* **2011**, *12*, 3077–3094.

(40) Peng, D.; Middendorf, N.; Weigend, F.; Reiher, M. An Efficient Implementation of Two-Component Relativistic Exact-Decoupling Methods for Large Molecules. *J. Chem. Phys.* **2013**, *138*, 184105.

(41) Liu, W.; Peng, D. Exact Two-Component Hamiltonians Revisited. *J. Chem. Phys.* **2009**, *131*, 031104.

(42) Peng, D.; Liu, W.; Xiao, Y.; Cheng, L. Making Four- and Two-Component Relativistic Density Functional Methods Fully Equivalent Based on the Idea of From Atoms to Molecule. *J. Chem. Phys.* **2007**, *127*, 104106.

(43) Xu, W.; Ma, J.; Peng, D.; Zou, W.; Liu, W.; Staemmler, V. Excited States of ReO_4^-: A Comprehensive Time-Dependent Relativistic Density Functional Theory Study. *Chem. Phys.* **2009**, *356*, 219–228.

(44) Xu, W.; Zhang, Y.; Liu, W. Time-dependent relativistic density functional study of Yb and YbO. *Sci. China Ser. B Chem.* **2009**, *52*, 1945–1953.

(45) Zhang, Y.; Xu, W.; Sun, Q.; Zou, W.; Liu, W. Excited States of OsO_4: A Comprehensive Time-Dependent Relativistic Density Functional Theory Study. *J. Comput. Chem.* **2010**, *31*, 532–551.

(46) Liu, W. Ideas of Relativistic Quantum Chemistry. *Mol. Phys.* **2010**, *108*, 1679–1706.

(47) Liu, W. Advances in Relativistic Molecular Quantum Mechanics. *Phys. Rep.* **2014**, *537*, 59–89.

(48) Liu, W. The Big Picture of Relativistic Molecular Quantum Mechanics. *Natl. Sci. Rev.* **2016**, *3*, 204–221.

(49) Sun, Q.; Xiao, Y.; Liu, W. Exact Two-Component Relativistic Theory for NMR Parameters: General Formulation and Pilot Application. *J. Chem. Phys.* **2012**, *137*, 174105.

(50) Heß, B. A.; Marian, C. M.; Wahlgren, U.; Gropen, O. A Mean-Field Spin-Orbit Method Applicable to Correlated Wavefunctions. *J. Chem. Phys.* **1996**, *251*, 365–371.

(51) Boettger, J. C. Approximate Two-Electron Spin-Orbit Coupling Term For Density-Functional-Theory DFT Calculations Using The Douglas-Kroll-Hess Transformation. *Phys. Rev. B* **2000**, *62*, 7809–7815.

(52) Neese, F. In *Calculation of NMR and EPR Parameters: Theory and Applications*; Kaupp, M., Bühl, M., Malkin, V. G., Eds.; Wiley-VCH Verlag GmbH & Co. KGaA, 2004; Chapter 31, pp 541–564.

(53) Rajagopal, A. K. Inhomogeneous Relativistic Electron Gas. *J. Phys. C Solid State* **1978**, *11*, L943–L948.

(54) MacDonald, A. H.; Vosko, S. H. A Relativistic Density Functional Formalism. *J. Phys. C Solid State* **1979**, *12*, 2977–2990.

(55) Saue, T.; Helgaker, T. Four-Component Relativistic Kohn-Sham Theory. *J. Comput. Chem.* **2002**, *23*, 814–823.

(56) Salek, P.; Helgaker, T.; Saue, T. Linear response at the 4-component relativistic

density-functional level: application to the frequency-dependent dipole polarizability of Hg, AuH and PtH_2. *Chem. Phys.* **2005**, *311*, 187–201.

(57) Capelle, K.; Vignale, G.; Györffy, B. Spin Currents and Spin Dynamics in Time-Dependent Density-Functional Theory. *Phys. Rev. Lett.* **2001**, *87*, 206403.

(58) Cao, Z.; Li, Z.; Wang, F.; Liu, W. Combining the Spin-Separated Exact Two-Component Relativistic Hamiltonian with the Equation-Of-Motion Coupled-Cluster Method for the Treatment of SpinOrbit Splittings of Light and Heavy Elements. *Phys. Chem. Chem. Phys.* **2017**, *19*, 3713–3721.

(59) Goings, J. J.; Ding, F.; Davidson, E. R.; Li, X. Approximate Singly Excited States from a Two-Component Hartree Fock Reference. *J. Chem. Phys.* **2015**, *143*, 144106.

(60) Seeger, R.; Pople, J. A. Self-consistent molecular orbital methods. XVIII. Constraints and stability in Hartree-Fock theory. *J. Chem. Phys.* **1977**, *66*, 3045–3050.

(61) Goings, J. J.; Ding, F.; Frisch, M. J.; Li, X. Stability of the Complex Generalized Hartree-Fock Equations. *J. Chem. Phys.* **2015**, *142*, 154109.

(62) Davidson, E. R. The Iterative Calculation of a Few of the Lowest Eigenvalues and Corresponding Eigenvectors of Real-Symmetric Matrices. *J. Comput. Phys.* **1975**, *17*, 87–94.

(63) Peng, B.; Lestrange, P. J.; Goings, J. J.; Caricato, M.; Li, X. Energy-Specific Equation-of-Motion Coupled-Cluster Methods for High-Energy Excited States: Application to K-Edge X-Ray Absorption Spectroscopy. *J. Chem. Theory Comput.* **2015**, *11*, 4146–4153, CHE-1265945,DE-AC02-06CH11357.

(64) Liang, W.; Fischer, S. A.; Frisch, M. J.; Li, X. Energy-Specific Linear Response TDHF/TDDFT for Calculating High-Energy Excited States. *J. Chem. Theory Comput.* **2011**, *7*, 3540–3547.

(65) Frisch, M. J.; Trucks, G. W.; Schlegel, H. B.; Scuseria, G. E.; Robb, M. A.; Cheeseman, J. R.; Scalmani, G.; Barone, V.; Mennucci, B.; Petersson, G. A.; Nakatsuji, H.; Caricato, M.; Li, X.; Hratchian, H. P.; Bloino, J.; Janesko, B. G.; Izmaylov, A. F.; Marenich, A.; Lipparini, F.; Zheng, G.; Sonnenberg, J. L.; Liang, W.; Hada, M.; Ehara, M.; Toyota, K.; Fukuda, R.; Hasegawa, J.; Ishida, M.; Nakajima, T.; Honda, Y.; Kitao, O.; Nakai, H.; Vreven, T.; Throssell, K.; Montgomery Jr., J. A.; Peralta, J. E.; Ogliaro, F.; Bearpark, M.; Heyd, J. J.; Brothers, E.; Kudin, K. N.; Staroverov, V. N.; Keith, T.; Kobayashi, R.; Normand, J.; Raghavachari, K.; Rendell, A.; Burant, J. C.; Iyengar, S. S.; Tomasi, J.; Cossi, M.; Rega, N.; Millam, J. M.; Klene, M.; Knox, J. E.; Cross, J. B.; Bakken, V.; Adamo, C.; Jaramillo, J.; Gomperts, R.; Stratmann, R. E.; Yazyev, O.; Austin, A. J.; Cammi, R.; Pomelli, C.; Ochterski, J. W.; Martin, R. L.; Morokuma, K.; Zakrzewski, V. G.; Voth, G. A.; Salvador, P.; Dannenberg, J. J.; Dapprich, S.; Parandekar, P. V.; Mayhall, N. J.; Daniels, A. D.; Farkas, O.; Foresman, J. B.; Ortiz, J. V.; Cioslowski, J.; ; Fox, D. J. Gaussian Development Version Revision I.04.

(66) Visscher, L.; Dyall, K. G. Dirac-Fock Atomic Electronic Structure Calculations Using Different Nuclear Charge Distributions. *At. Data Nucl. Data Tables* **1997**, *67*, 207–224.

(67) Quiney, H. M.; Laerdahl, J. K.; Fægri, Jr., K.; Saue, T. Ab Initio Dirac-Hartree-Fock Calculations of Chemical Properties and PT-Odd Effects in Thallium Fluoride. *Phys. Rev. A* **1998**, *57*, 920–944.

(68) Hohenberg, P.; Kohn, W. Inhomogeneous Electron Gas. *Phys. Rev.* **1964**, *136*, B864–B871.

(69) Vosko, S. H.; Wilk, L.; Nusair, M. Accurate Spin-Dependent Electron Liquid Correlation Energies for Local Spin Density Calculations: a Critical Analysis. *Can. J. Phys.* **1980**, *58*, 1200–1211.

(70) Becke, A. D. Density-Functional Exchange-Energy Approximation with Correct Asymptotic Behavior. *Phys. Rev. A* **88**, *38*, 3098–3100.

(71) Lee, C.; Yang, W.; Parr, R. G. Development of the Colle-Salvetti correlation-energy formula into a functional of the electron density. *Phys. Rev. B* **1988**, *37*, 785–789.

(72) Miehlich, B.; Savin, A.; Stoll, H.; Preuss, H. Results Obtained with the Correlation Energy Density Functionals of Becke and Lee, Yang and Parr. *Chem. Phys. Lett.* **1989**, *157*, 200–206.

(73) Becke, A. D. Density-functional thermochemistry. III. The role of exact exchange. *J. Chem. Phys.* **1993**, *98*, 5648–5652.

(74) Perdew, J. P.; Burke, K.; Ernzerhof, M. Generalized Gradient Approximation Made Simple. *Phys. Rev. Lett.* **1996**, *77*, 3865–3868.

(75) Adamo, C.; Barone, V. Toward reliable density functional methods without adjustable parameters: The PBE0 model. *J. Chem. Phys.* **1999**, *110*, 6158–6169.

(76) Tao, J.; Perdew, J. P.; Staroverov, V. N.; Scuseria, G. E. Climbing the Density Functional Ladder: Nonempirical MetaGeneralized Gradient Approximation Designed for Molecules and Solids. *Phys. Rev. Lett.* **2003**, *91*, 146401.

(77) Zhao, Y.; Truhlar, D. G. The M06 suite of density functionals for main group thermochemistry, thermochemical kinetics, noncovalent interactions, excited states, and transition elements: two new functionals and systematic testing of four M06-class functionals and 12 other functionals. *Theor. Chem. Acc.* **2008**, *393*, 215–241.

(78) Zhao, Y.; Truhlar, D. G. Comparative DFT Study of van der Waals Complexes: Rare-Gas Dimers, Alkaline-Earth Dimers, Zinc Dimer, and Zinc-Rare-Gas Dimers. *J. Phys. Chem. A* **2006**, *110*, 5121–5129.

(79) Zhao, Y.; Truhlar, D. G. Density Functional for Spectroscopy: No Long-Range Self-Interaction Error, Good Performance for Rydberg and Charge-Transfer States, and Better Performance on Average than B3LYP for Ground States. *J. Phys. Chem. A* **2006**, *110*, 13126–13130.

(80) Das, G.; Wahl, A. C. Extended Hartree-Fock Wavefunctions: Optimized Valence Configurations for H_2 and Li_2, Optimized Double Configurations for F_2. *J. Chem. Phys.* **1966**, *44*, 87–96.

(81) Kutzelnigg, W.; Staemmler, V. Potential Curve of the Lowest Triplet State of Li_2. *Chem. Phys. Lett.* **1972**, *13*, 496–500.

(82) Schmidt-Mink, I.; Müller, W.; Meyer, W. Ground- and Excited-State Properties of Li_2 and Li_2^+ from Ab Initio Calculations with Effective Core Polarization Potentials. *Chem. Phys.* **1985**, *92*, 0301–0104.

(83) Olson, M. L.; Konowalow, D. D. The Potential Energy Curve for the $B_1\Pi_u$ state of Li_2. *Chem. Phys. Lett.* **1976**, *39*, 281–284.

(84) Konowalow, D. D.; Fish, J. L. *Chem. Phys.* **1984**, *84*, 463–475.

(85) A. Pashov, W. J.; Kowalczyk, P. The Li_2 $F^1\Sigma_g^+$ "shelf" State: Accurate Potential Energy Curve Based on the Inverted Perturbation Approach. *J. Chem. Phys.* **2000**, *113*, 6624–6627.

(86) W. Jastrzbski, A. P.; Kowalczyk, P. The $F^1\Sigma_g^+$ state of lithium dimer revised. *J. Chem. Phys.* **2001**, *114*, 10725–10727.

(87) Musiał, M.; Kucharski, S. A. First Principle Calculations of the Potential Energy Curves for Electronic States of the Lithium Dimer. *J. Chem. Theory Comput.* **2014**, *10*, 1200–1211.

(88) Jasik, P.; Sienkiewicz, J. E. *Chem. Phys.* **2006**, *323*, 563–573.

(89) Poteau, R.; Spiegelmann, F. *J. Mol. Spectrosc.* **1995**, *171*, 299–308.

(90) Müuller, W.; Meyer, W. *J. Chem. Phys.* **1984**, *80*, 3311–3320.

(91) Minaev, B. *Spectrochim. Acta A* **2005**, *62*, 790–799.

(92) Kaldor, U. *Chem. Phys.* **1990**, *140*, 1–6.

(93) Musiał, M.; Kowalska-Szojda, K.; Lyakh, D. I.; Bartlett, R. J. *J. Chem. Phys.* **2013**, *138*, 194103.

(94) Shi, D.-H.; Ma, H.; Sun, J.-F.; Zhu, Z.-L.; Liu, Y.-F.; Yu, B.-H. *J. Mol. Struct.: THEOCHEM* **2007**, *824*, 71–75.

(95) Ipatov, A.; Cordova, F.; Doriol, L. J.; Casida, M. E. Excited-State Spin-Contamination in Time-Dependent Density-Functional Theory for Molecules with Open-Shell Ground States. *J. Mol. Struct.: THEOCHEM* **2009**, *914*, 60–73.

(96) Noro, T.; Sekiya, M.; Koga, T. Segmented Contracted Basis Sets for Atoms H through Xe: Sapporo-(DK)-nZP Sets (n = D, T, Q). *Theor. Chem. Acc.* **2012**, *131*, 1124.

(97) Thompson, T. C.; Truhlar, D. G.; ; Mead, C. A. On the Form of the Adiabatic and Diabatic Representation and the Validity of the Adiabatic Approximation for X_3 Jahn-Teller Systems. *J. Chem. Phys.* **1985**, *82*, 2392–2405.

(98) Martins, J. L.; Car, R.; Buttet, J. Electronic Properties of Alkali Trimers. *J. Chem. Phys.* **1983**, *78*, 5646–5655.

(99) Thompson, T. C.; Izmirlian, Jr., G.; Lemon, S. J.; Truhlar, D. G.; Mead, C. A. Consistent Analytic Representation of the Two Lowest Potential Energy Surfaces for Li_3, Na_3, and K_3. *J. Chem. Phys.* **1985**, *82*, 5597–5603.

(100) Ehara, M.; Yamashita, K. Theoretical Studies of the Potential Energy Surface and Wavepacket Dynamics of the Li_3 System. *Theor. Chem. Acc.* **1999**, *102*, 226–236.

(101) Ghassemi, E. N.; Larson, J.; Larson, Å. A Diabatic Representation of the Two Lowest Electronic States of Li_3. *J. Chem. Phys.* **2014**, *140*, 154304.

(102) Sadygov, R. G.; Yarkony, D. R. Unusual Conical Intersections in the Jahn-Teller Effect: The Electronically Excited States of Li_3. *J. Chem. Phys.* **1999**, *110*, 3639–3642.

(103) Hammes-Schiffer, S.; Andersen, H. C. Ab Initio and Semiempirical Methods for Molecular Dynamics Simulations Based on General Hartree-Fock Theory. *J. Chem. Phys.* **1993**, *99*, 523–532.

(104) Hirshfeld, F. L. Bonded-atom fragments for describing molecular charge densities. *Theor. Chem. Acc.* **1977**, *44*, 129.

(105) Lynch, D.; Herman, M. F.; Yeager, D. L. Excited State Properties from the Equations of Motion Method. Application of the MCTDHF-MCRPA to the Dipole Moments and Oscillator Strengths of the $A^1\Pi$, $a'^3\Pi$, $a'^3\Sigma^+$ and $d^3\Delta$ Low-Lying Valence States of CO. *Chem. Phys.* **1982**, *64*, 69–81.

(106) Casida, M. E. Time-Dependent Density-Functional Theory for Molecules and Molecular Solids. *J. Mol. Struct.: THEOCHEM* **2009**, *914*, 3–18.

(107) Cui, Y.; Bulik, I. W.; Jiménez-Hoyos, C. A.; Henderson, T. M.; Scuseria, G. E. Proper and improper zero energy modes in Hartree-Fock theory and their relevance for symmetry breaking and restoration. *J. Chem. Phys.* **2013**, *139*, 154107.

(108) Li, X.; Smith, S. M.; Markevitch, A. N.; Romanov, D. A.; Levis, R. J.; Schlegel, H. B. A Time-Dependent Hartree-Fock Approach for Studying the Electronic Optical Response of Molecules in Intense Fields. *Phys. Chem. Chem. Phys.* **2005**, *7*, 233–239.

(109) Isborn, C. M.; Li, X.; Tully, J. C. TDDFT Ehrenfest Dynamics: Collisions between Atomic Oxygen and Graphite Clusters. *J. Chem. Phys.* **2007**, *126*, 134307.

(110) Liang, W.; Chapman, C. T.; Li, X. Efficient First-Principles Electronic Dynamics. *J. Chem. Phys.* **2011**, *134*, 184102.

(111) Bruner, A.; LaMaster, D.; Lopata, K. Accelerated Broadband Spectra using Transition Dipole Decomposition and Padé Approximants. *J. Chem. Theory Comput.* **2016**, *12*, 3741–3750.

(112) Pierloot, K.; van Besien, E.; van Lenthe, E.; Baerends, E. J. Electronic Spectrum of UO_2^{2+} and $[UO_2Cl_2]^{2-}$ Calculated with Time-Dependent Density Functional Theory. *J. Chem. Phys.* **2007**, *126*, 194311.

(113) Réal, F.; Vallet, V.; Marian, C.; Wahlgren, U. Theoretical Investigation of The Energies and Geometries of Photoexcited Uranyl(VI) Ion: A Comparison Between Wave-Function Theory and Density Functional Theory. *J. Chem. Phys.* **2007**, *127*, 214302.

(114) Zhang, Z.; Pitzer, R. M. Application of Relativistic Quantum Chemistry to the Electronic Energy Levels of the Uranyl Ion. *J. Phys. Chem. A* **1999**, *103*, 6880–6886.

(115) Pierloot, K.; van Besien, E. Electronic Spectrum and Spectrum of UO_2^{2+} and $[UO_2Cl_2]^{2-}$. *J. Chem. Phys.* **2005**, *123*, 204309.

(116) Tecmer, P.; Gomes, A. S. P.; Knecht, S.; Visscher, L. Communication: Relativistic Fock-Space Coupled Cluster Study of Small Building Blocks of Larger Uranium Complexes. *J. Chem. Phys.* **2014**, *141*, 041107.

(117) Kendall, R. A.; Dunning Jr., T. H.; Harrison, R. J. Electron affinities of the first-row atoms revisited. Systematic basis sets and wave functions. *J. Chem. Phys.* **1992**, *96*, 6796–6806.

(118) Pantazis, D. A.; Neese, F. All-electron scalar relativistic basis sets for the actinides. *J. Chem. Theory Comput.* **2011**, *7*, 677–684.

Graphical TOC Entry